Atmos. Chem. Phys. Discuss., 14, 7965–8013, 2014
www.atmos-chem-phys-discuss.net/14/7965/2014/
doi:10.5194/acpd-14-7965-2014

Atmospheric Chemistry and Physics Discussions

Airborne flux measurements of biogenic volatile organic compounds over California

P. K. Misztal[1,2], T. Karl[2,*], R. Weber[1], H. H. Jonsson[3], A. B. Guenther[2,], and A. H. Goldstein[1]**

[1]University of California at Berkeley, Berkeley, California, USA
[2]National Center for Atmospheric Research, Boulder, Colorado, USA
[3]Center for Interdisciplinary Remotely-Piloted Aircraft Studies, Monterey, California, USA
[*]now at: Institute for Meteorology and Geophysics, University of Innsbruck, Innsbruck, Austria
[**]now at: Atmospheric Sciences and Global Change Division, Pacific Northwest National Laboratory, Richland, Washington, USA

Received: 30 January 2014 – Accepted: 11 March 2014 – Published: 24 March 2014

Correspondence to: P. K. Misztal (pkm@berkeley.edu)

Published by Copernicus Publications on behalf of the European Geosciences Union.

Abstract

Biogenic Volatile Organic Compound (BVOC) fluxes were measured onboard the CIRPAS Twin Otter aircraft as part of the California Airborne BVOC Emission Research in Natural Ecosystem Transects (CABERNET) campaign during June 2011. The airborne virtual disjunct eddy covariance (AvDEC) approach used measurements from a PTR-MS and a wind radome probe to directly determine fluxes of isoprene, MVK + MAC, methanol, monoterpenes, and MBO over ~ 10 000 km of flight paths focusing on areas of California predicted to have the largest emissions of isoprene. The Fast Fourier Transform (FFT) approach was used to calculate fluxes over long transects of more than 15 km, most commonly between 50 and 150 km. The Continuous Wavelet Transformation (CWT) approach was used over the same transects to also calculate "instantaneous" fluxes with localization of both frequency and time independent of non-stationarities. Vertical flux divergence of isoprene is expected due to its relatively short lifetime and was measured directly using "racetrack" profiles at multiple altitudes. It was found to be linear and in the range 5 % to 30 % depending on the ratio of aircraft altitude to PBL height (z/z_i). Fluxes were generally measured by flying consistently at 400 ± 50 m (a.g.l.) altitude, and extrapolated to the surface according to the determined flux divergence. The wavelet-derived surface fluxes of isoprene averaged to 2 km spatial resolution showed good correspondence to Basal Emission Factor (BEF) landcover datasets used to drive biogenic VOC (BVOC) emission models. The surface flux of isoprene was close to zero over Central Valley crops and desert shrublands, but was very high (up to 15 mg m^{-2} h^{-1}) above oak woodlands, with clear dependence of emissions on temperature and oak density. Isoprene concentrations of up to 8 ppb were observed at aircraft height on the hottest days and over the dominant source regions.

While isoprene emissions from agricultural crop regions, shrublands, and coniferous forests were extremely low, high concentrations of methanol and monoterpenes were found above some of these regions.

ACPD
14, 7965–8013, 2014

These observations demonstrate the ability to measure fluxes from specific sources by eddy covariance from an aircraft, and suggest the utility of measurements using fast response chemical sensors to constrain emission inventories and map out source distributions for a much broader array of trace gases than was observed in this study.

This paper reports the first regional direct eddy covariance fluxes of isoprene. The emissions of VOCs measured from aircraft with 2 km spatial resolution can quantify the distribution of major sources providing the observations required for testing statewide emission inventories of these important trace gases. These measurements will be used in a future study to assess BVOC emission models and their driving variable datasets.

1 Introduction

Volatile Organic Compounds (VOCs) play important roles in atmospheric chemistry such as fueling tropospheric ozone production, forming secondary organic aerosols, and acting as important radical sinks in regions near sources. The global annual source strength of gas-phase biogenic volatile organic compounds (BVOC) is around 1 Pg (10^{15} g) (Guenther et al., 2012). One half of these mass emissions (500 Tg) is constituted by a single highly reactive hemiterpene, isoprene (2-methyl-1,3-butadiene). The other half is represented by hundreds to thousands of compounds which span the atmospheric lifetime ranges from a few seconds (e.g. sesquiterpenes) to months (e.g. benzene), and are actively exchanged in both directions (emission and deposition) between the biosphere and atmosphere (Park et al., 2013). Currently, BVOC measurements (mostly of emission) have been reported at ecosystem scales primarily from fixed tower sites which offer very good temporal resolution, but lack spatial resolution across the broader landscape that is critical for understanding regional photochemistry.

Since the discovery of substantial isoprene emissions from forested regions (Rasmussen, 1970), and subsequent progress in understanding isoprene biochemistry (Loreto and Sharkey, 1990), much research has been conducted to understand the emissions of isoprene and the factors that drive them at the leaf level, including in Cal-

ACPD
14, 7965–8013, 2014

ifornia (Arey et al., 1991a, b, 1995; Baker et al., 1999; Karlik and Winer, 2001; Kurpius and Goldstein, 2003; Goldstein and Schade, 2000; Schade et al., 1999, 2000; Schade and Goldstein, 2001; Winer et al., 1992). This work has led to BVOC emission models such as BEIS (Pierce et al., 1998), MEGAN (Guenther et al., 2012) and BEIGIS (Scott and Benjamin, 2003) that are driven by information about weather conditions, plant distributions, leaf area, and the temperature and light response of isoprene emissions from plants. There have been isoprene flux measurements at the canopy scale in a variety of locations worldwide: Northwestern US oak savanna (Lamb et al., 1986), Northeastern US mixed forest (Goldstein et al., 1998), North Central US mixed forest (Westberg et al., 2001; Apel et al., 2002), Amazonian tropical forests (Rinne et al., 2002; Kuhn et al., 2002), Central Africa rainforest (Serca et al., 2001), Borneo rainforest (Langford et al., 2010), etc. However, in California, no ecosystem scale fluxes have ever been reported for an oak dominated ecosystem that could be used to verify the modeled statewide isoprene emission inventory.

A California BVOC model called BEIGIS (Scott and Benjamin, 2003) predicts significant emissions of isoprene from oak woodlands distributed throughout the foothills of the Coast Range and the Sierra Nevada mountains (Fig. 1a). However, with the exception of a single site in a pine plantation (Schade et al., 1999, 2000; Schade and Goldstein, 2001; Goldstein and Schade, 2000), and measurements in a few crops (Karl et al., 2008; Fares et al., 2011; Fares et al., 2012; Park et al., 2013), there have been no measurements of BVOC fluxes from California landscapes at a larger spatial scale than individual leaves and branches. The goal of our work was to measure the distribution of isoprene flux across the oak woodland areas of California in order to test and improve the landscape-scale emission models that are used for regional air quality assessments. California is a region where these observations are particularly needed because of its varied landscape, with BVOC emissions from biogenic areas dominated by Oaks (~ 7 % of land area), and with anthropogenic VOC emissions from the activity of ~ 35 million people living in the state. Furthermore, the accuracy of isoprene emission estimates is important for regional simulations of ozone production.

ACPD
14, 7965–8013, 2014

Although the vast majority of eddy covariance measurements have been conducted on the ground, Airborne Eddy Covariance (AEC) is an established technique which has been used extensively in the last several decades to measure fluxes (e.g. of energy, ozone, carbon dioxide, etc.) directly using an aircraft (e.g. Lenschow et al., 1981; Desjardins et al., 1992; Pattey et al., 2002; Metzger et al., 2013). The first successful implementation of AEC for VOC was by Karl et al. (2009) over Mexico using a C130 aircraft.

In this paper, we present the first regional BVOC flux measurements focused on transects over areas expected to dominate BVOC emissions in California. Vertical "racetrack" profiles were used for testing the flux methodology and derivation of flux divergence terms, which were recently described in a separate paper (Karl et al., 2013) where we demonstrated that our PTR-MS configuration in CABERNET was appropriate for measuring isoprene fluxes.

We report the observed spatial distribution of airborne fluxes and emission factors and demonstrate that they match well the emission factors from landcovers estimated using a California Air Resources Board implementation of the MEGAN model. The data will be more thoroughly explored in a separate modeling paper focused on improving landcover databases and accuracy of VOC inventories in California.

The motivation for conducting this regional flux study in California was driven by: (1) the need for spatially resolved data on BVOC emissions from oak woodlands which have a large impact on regional ozone concentrations, and (2) our lack of information on how BVOC emissions respond to variations in landcover (plant functional type distributions, LAI, etc).

ACPD
14, 7965–8013, 2014

2 Methodology

2.1 Study region

Oaks are the main source of isoprene in California and they grow dominantly in certain elevations (400–800 m) along the foothills encompassing the Central Valley and along the Coastal Range Mountains. These specific locations, relatively constant elevations, and high emission rates make oaks an ideal subject for flux observations from aircraft. Using the USGS National Gap Analysis Program (GAP) landcover database, we planned our survey flights (to measure surface fluxes over long transects at constant altitude) and racetrack flights at several levels (vertical profiles to characterize flux divergence) over more or less homogeneous oak woodlands consisting of the Blue Oak Woodlands (BOW), Valley Oak Woodlands (VOW) and Coastal Oak Woodlands (COW). The total percentage of the sum of their primary, secondary and tertiary levels was used to map out the most homogeneous areas where oaks are the only or the dominating tree species (see Sect. 2.3 on flight track planning). Despite this biological homogeneity the oaks have highly irregular distribution patterns characterized by varying spatial densities. Figure S1 shows a typical oak ecosystem as seen from the Twin Otter flying over Tonzi Ranch tower, where ground flux measurements of isoprene were simultaneously performed for comparison with the aircraft observations (see Sect. 3.2.2). Apart from relatively homogeneous (in terms of the species) oak woodlands mostly in the foothill bands, further away there are transition areas with coniferous regions where, according to the GAP database, the oaks grade in to Blue Oak – Ponderosa Pine (BOP) habitats and/or Montane Hardwood-Conifer (MHC), and/or Montane Hardwood (MHW). These areas are represented in Fig. 1b.

2.2 Climatology during field campaign

Environmental context is important to take into account when analyzing measured BVOC fluxes because the history of temperature and photosynthetically active radi-

ACPD
14, 7965–8013, 2014

ation (PAR) is the main driver of potential vegetative emissions (Sharkey et al., 1999; Fuentes and Wang, 1999), and seasonal variability in climate is known to affect gross ecosystem production in this region (Goldstein et al., 2000). The climatological conditions in California in June 2011 were relatively colder than in June of the previous year. The preceding month and the first week of June 2011 were particularly cold followed by gradual increase in the temperature throughout the campaign with particularly hot sunny weather on the final flight of the campaign. Along with the warming, the environment was becoming dryer.

2.3 Flight track planning

The CABERNET airborne campaign took place in June 2011. The paths of the research survey flights and "racetrack" gradient flights are portrayed over the BEIGIS isoprene emission factor map (Fig. 1a) and California map of oak woodland distribution (Fig. 1b). Weather forecasting was used to ensure that all the flights were conducted on cloudless days, and where possible for the mean wind direction to be perpendicular to the flight paths. A test flight on 1 June was performed over the ocean to calibrate the sensors using pitch and yaw maneuvers, according to Lenschow (1986). These were used to test the accuracy of coefficients for wind vector transformations to ensure the vertical wind speed is not affected by aircraft motion. More detailed information on these maneuvers made during CABERNET can be found in Karl et al. (2013).

The true air speed (TAS) was kept as constant as possible on all the flights. For the entire campaign the TAS ranged from around 52 to 67 $m\,s^{-1}$ with an average of 58 $m\,s^{-1}$, and a standard deviation of 2.3 $m\,s^{-1}$. The measured air temperature at aircraft altitude ranged from 19.4 to 25.9 °C (mean: 22.5 °C, s.d.: 1.28 °C) while the temperature at 2 m above the surface (WRF model) was wider in range (from 10.9 to 34.8 °C) and higher by 3.6 °C average temperature.

The available forty hours of flight time was divided into eight research flights (RF) which were carried out for approximately 4–5 h each during the mid-day. The individual flown tracks are described in Sects. 2.3.1 to 2.3.8.

ACPD
14, 7965–8013, 2014

Summary information specific to planning of each research flight (RF) is provided in Table 1.

2.3.1 RF 1 – 8 June

Research flight 1 occurred on the coolest (but still clear) day of the field study and passed to the WSW across the Central Valley, then above the most southern segment of the oak band of the Sierra Nevada foothills and further towards the shrublands of the Mojave Desert. The returning leg diagonally cut through some of the more polluted regions of the Central Valley, passing over oil fields, dairies and other anthropogenic VOC sources. It may be relevant that the preceding period prior to 8 June was particularly cold so the biogenic emission capacity was expected to be increasing on this flight and the flight the next day. The VOCs measured included some anthropogenic VOC mass-to-charge ratios (m/z) not measured in other flights, comprised of isoprene (m/z 69), methanol (m/z 33), benzene (m/z 79), toluene (m/z 93) and C-8 aromatics (C2-benzenes, benzaldehyde) (m/z 107).

2.3.2 RF 2 – 9 June

Research flight 2 occurred during cool-weather and measured fluxes to the north east passing near the Walnut Grove tower (WGC), Tonzi Ranch Tower (TRT) and the Blodgett Forest site (BF). This flight continued up to 40° N latitude of the northern Sierra Nevada foothill oak band and returned on the same path providing data near the WGC, TRT and BF sites located approximately half way and seen by the aircraft twice over a 2 h period. The region covered by this RF overlapped about 50 % with RF 3 and 4. The compounds measured included: isoprene (m/z 69), methyl vinyl ketone and methacrolein (MVK + MACR) (m/z 71), methanol (m/z 33), monoterpenes (m/z 81, 137), and methyl butenol (MBO) (m/z 87).

ACPD
14, 7965–8013, 2014

2.3.3 RF 3 – 10 June

Half of research flight 3 was spent doing the first vertical "racetrack" profile flight, and the rest was devoted to segments overlapping spatially with the ground-based towers (WGC and TRT) and with RF 2 and 4. The racetrack legs were relatively long in order to oversample and then determine the optimal track lengths for wavelet flux determination with this particular aircraft. Targeted compounds were isoprene (m/z 69), MVK + MACR (m/z 71), hydroxyacetone (m/z 75), and methanol (m/z 33).

2.3.4 RF 4 – 14 June

Research flight 4 was a survey that shared the same initial route to the San Joaquin Delta as the two previous flights and after reaching the Sierra foothills it continued South right over the oak woodlands until intersection with the route used in RF1. This provided extensive coverage of a portion of the oaks on the eastern edge of the Central Valley. The return flight followed the same path until reaching Bakersfield to the left and then proceeded straight across the Central Valley above some of the many dairies in the region. Isoprene (m/z 69), MVK + MACR (m/z 71), methanol (m/z 33), monoterpenes (m/z 81, 137), and MBO (m/z 87) were the measured compounds.

2.3.5 RF 5 – 15 June

Research flight 5 went to the North through the San Francisco Bay Area and near Santa Rosa to measure emissions from oak woodlands in the coastal regions. After reaching the most northern point the plane flew towards the San Joaquin Delta region near rice paddies. A biomass burning episode from one rice field was explored with the aircraft to observe methanol, acetaldehyde, and possibly furan (see Supplement video). Measured compounds were isoprene (m/z 69), MVK + MACR (m/z 71), methanol (m/z 33), monoterpenes (m/z 81, 137), and acetaldehyde (m/z 45).

ACPD
14, 7965–8013, 2014

2.3.6 RF 6 – 16 June

Research flight 6 was focused on flying a stack of racetracks over relatively homogeneous oak terrain in the Sierra foothills near Madera. The racetrack consisted of 5 sequential segment lengths of 15 km at evenly distributed altitudes within the PBL. The racetrack started at the top level directly following a saw-tooth sounding. The plane performed one lap at each height on the decent and again on the ascent. When the top level was reached another saw-tooth sounding was performed and the whole racetrack sequence was repeated. Since this paper is focused on the results from survey transects, the reader is referred for details of vertical profile racetrack results to Karl et al. (2013). Just three masses were measured: isoprene (m/z 69), MVK + MACR (m/z 71), and MBO (m/z 87).

2.3.7 RF 7 – 20 June

Research flight 7 was also focused on racetrack profiles and was situated in a similar location to the racetrack in RF 6, but was rotated for the predicted wind direction to be perpendicular to the straight side of the track. One main difference was that this racetrack saw higher temperatures than RF6 four days earlier which was reflected in observed higher concentrations. However, the flux divergence terms obtained from both racetracks 6 and 7 were very similar. The measured masses corresponded to the following targeted compounds: isoprene (m/z 69), MVK + MACR (m/z 71), and hydroxyacetone (m/z 75).

2.3.8 RF 8 – 21 June

Research flight 8 was a survey towards the south of Monterey covering the coastal oak savannahs during the hottest day of all RFs. While in previous flights concentrations of a few ppb of isoprene were observed, the instantaneous maximal concentrations in this RF reached 8 ppb. The following compounds were targeted on this flight: isoprene

ACPD
14, 7965–8013, 2014

(m/z 69), MVK + MACR (m/z 71), methanol (m/z 33), monoterpenes (m/z 137), and MBO (m/z 87).

2.4 Aircraft

A two-engine UV-18A Twin Otter (the military version of model Series 300) research aircraft was operated by the Center for Interdisciplinary Remote Piloted Aircraft Study (CIRPAS) of the Naval Postgraduate School out of the airport located in Marina, CA near Monterey, CA. The aircraft is equipped with micrometeorological sensors and is capable of flux measurements (Karl et al., 2013). Air was drawn from a 3-inch isokinetic pipe inlet extending above the nose of the plane. Ambient air gets diffused from a 2.047 inch ID orifice at the tip (area ratio of about 2) to another diffuser with an area ratio of 5, resulting in a flow speed inside the tube of about 10 % of the aircraft speed ($\sim 60\,\mathrm{m\,s^{-1}}$). The vertical wind speed in the airplane coordinate system was measured by a five-hole radome probe with 33° half-angles at the nose of the aircraft. The vertical wind speed with respect to the earth is obtained from this measured vertical wind speed corrected for airplane motions measured by an inertial reference unit. The measured vertical wind speed is unaffected by the aircraft movement and flow distortion at the nose, as long as corrections based on "Lenschow maneuvers" are applied (Lenschow, 1986). More detailed descriptions of this particular aircraft can be found elsewhere (Hegg et al., 2005; Reid et al., 2001).

The aircraft payload is relatively large allowing for an extensive set of instrumentation and between 1 and 3 research crew on board. The list of instrumentation included: (1) NCAR's airborne PTR–MS for VOC fluxes; (2) an adsorbent-cartridge automatic sampler for GC-MS VOC speciation and validation of contributions to m/z measured by the PTR-MS; (3) a Picarro 2 Hz methane/CO2 analyzer; (4) a slow ozone analyzer (2B Tech) and dry chemo-luminescent fast-ozone sensor (NOAA); and (5) a water-based Condensation Particle Counter (CPC, TSI Inc.).

The VOC cartridge sampler containing 8 adsorbent tubes was manually activated during the flight and was recorded by a datalogger analog input to mark the timing of

ACPD
14, 7965–8013, 2014

each sample, which was drawn automatically through the cartridge for 8 min at a constant flow of 335 standard cubic centimeters per minute (sccm). In addition, one tube served as a blank for each flight and one tube was kept open inside the cabin for passive absorption of VOCs present in the cabin air to help in the identification of potential tube leaks.

2.5 Proton Transfer Reaction Mass Spectrometry (PTR-MS)

The Proton Transfer Reaction Mass Spectrometer (PTR-MS) is a fast sensor which can measure concentrations of VOC in a high frequency (10 Hz) virtual disjunct mode (Karl et al., 2002). Unlike a disjunct sampler which rapidly grabs a sample periodically, a PTR-MS instrument can be regarded as a virtual disjunct sampler where the ambient air is sampled continuously but m/z are analyzed sequentially by the quadrupole detector, creating a disjunct dataset with high frequency data (e.g. 10 Hz) separated by a relatively longer gap (e.g. 2 Hz).

The instrument deployed in CABERNET was NCAR's high sensitivity PTR-MS (Karl et al., 2009). Its internal vacuum inlet system was specifically redesigned to enable stable operation across a wide range of altitudes and to ensure internal lag-time of less than 100 ms. The instrument operation and routine were kept consistent for each flight. Current FAA regulations do not allow for the instrumentation to be running overnight, requiring specific steps to achieve stable instrument operation quickly after an instrument start-up. A flight-optimized vacuum system and internal capillary components result in fast transfer time from the inlet to the drift tube and independence of ambient pressure variations on the drift-tube pressure at high altitudes. The valves between the water reservoir and the ion source reduce the time to achieve ion source stability and low oxygen ion levels in the drift tube. Approximately three hours before the take-off the instrument was powered up, and approximately 1 h before the take-off, if the O_2^+ signal went below 6 % of the primary ions, a secondary electron multiplier (SEM) and ion source check with optimization was followed by a dynamic calibration using two VOC standards (Apel–Riemer), one high concentration (available

ACPD
14, 7965–8013, 2014

during pre-flight) containing low-fragmenting compounds for daily sensitivity curves (i.e. benzene (1.11 ppm), toluene (1.07 ppm), xylenes (4.22 ppm), trimethylbenzene (1.94 ppm), dichlorobenzene (2.61 ppm), and trichlorobenzene (1.14 ppm)) diluted with VOC-free air and another low-concentration standard containing isoprene (10.0 ppb) (also available in-flight) which was also used as a back-flushing gas during the take-offs and touch-downs to prevent the exhaust plumes from contaminating the inlet. Zeros were measured using three different sources: Pt-catalyzed ambient air; ultra-pure compressed air (Air Liquide); ambient air at the top of the tooth sounding well above the PBL height. The calibrated normalized sensitivities for calibrated VOCs experienced day-to-day variabilities of less than 30 %. The average sensitivity for isoprene was 15.1 normalized counts per second per ppbv (ncps ppbv^{-1}) as a sum of m/z 69 (13.4 ncps ppbv^{-1}) and m/z 41 (2.2 ncps ppbv^{-1}). The m/z 41 ion was used to assess the stability of isoprene fragmentation but only m/z 69 was used in the calculation of concentrations. These sensitivities resulted in detection limits of less than 10 pptv for isoprene corresponding to one km of flight. The primary ion count rates monitored at m/z 21 were around 2.0×10^7 counts per second (cps) (±20 %) so the absolute sensitivities were approximately 20 times higher than the normalized sensitivities (i.e. ∼ 300 cps ppbv^{-1} for isoprene). The sensitivities for compounds not present in the standard were approximated for each day from combining sensitivity curves of the daily calibrations with sensitivity curves from post-campaign calibrations using several different standards at a range of humidities. The accuracy of sensitivities was estimated at ±10 % for direct calibration (5 % standard certification + 5 % from dilution) and ±30 % for the approach combining post-campaign calibrations. The settings, sensitivities and further methodological remarks are included in Supplement Table S2.

2.6 Airborne eddy covariance (AEC)

The preferred micrometeorological method for measuring trace gas fluxes in the turbulent boundary layer is eddy covariance (EC). This approach is a direct measurement of the fluctuating vertical wind velocity and trace gas concentration. The flux is deter-

ACPD
14, 7965–8013, 2014

mined from the mean covariance between vertical wind velocity (w) and concentration (c) fluctuations and can be expressed as

$$F = \overline{w'c'} \quad (1)$$

where w' is the difference between the instantaneous and mean vertical wind speed and c' is the difference between the instantaneous and mean trace gas concentration. Here we use $w'c'$ to represent the time average of the product of these two variables. The major components of an EC flux system are: (1) a system that measures vertical wind speed with a fast (typically < 100 ms) response time; (2) an instrument that measures the targeted atmospheric constituent with a fast response time; and (3) a system to receive and store the data (e.g, datalogger or computer). Instruments with slower (> 100 ms) response times can be used to measure the flux associated with lower frequencies but may underestimate the total flux depending on the frequency of the eddies. In some cases this may result in an acceptable error while in other cases an attempt can be made to account for the loss of flux due to inadequate sensor response (Moore, 1986; Rowe et al., 2011). One way for estimating high frequency correction involves using another scalar that is measured with a fast response sensor and then estimating the reduction in flux that results if a digital filter is used to simulate response time of the slower instrument.

EC is used extensively to measure sensible and latent heat fluxes, and has recently been used for networks dedicated to quantifying carbon dioxide fluxes from various landscapes (Baldocchi, 2003). Commercial fast response instruments are available for some compounds (e.g. CO_2, H_2O, CH_4) and others can be built for additional chemical species. EC is generally preferred as the most direct flux measurement method which does not require parameterizations. Fluxes of VOC with short lifetimes can be estimated from flux divergence measurements (Lenschow et al., 1980).

Wyngaard and Brost (1984) proposed that the surface fluxes could also be estimated from measurements of vertical concentration profiles in the daytime mixed boundary layer (MBL) that lies above the surface layer and can extend up to several km. This

ACPD
14, 7965–8013, 2014

method assumes that the mean vertical gradient of a VOC in the MBL is determined by the depth of the MBL (z_i), the convective velocity scale (w^*), and the fluxes at the bottom and the top of the MBL. We used vertical profiles of temperature and humidity measured during "saw-tooth soundings" (steep climbs through PBL and part of the free troposphere (e.g. up to 3 km) at a constant angle followed by the similarly steep descent) to directly characterize z_i and measured sensible heat fluxes to quantify w^*. The MBL gradient-flux technique assumes that boundary layer mixing is dominated by convective turbulence and that boundary layer conditions evolve slowly compared to the convective turnover time of about 10 min. The results are not affected by vertically homogeneous horizontal advection or time dependence in the mean concentration and the method can account for entrainment.

A time scale at a fixed point in the PBL can be related to a length scale by multiplying the time scale by the average wind speed, as long as the "frozen turbulence" hypothesis known as Taylor's hypothesis (e.g. Panofsky and Dutton, 1984) is fulfilled. This hypothesis enables approximate conversion from temporal to spatial statistics. Since aircraft can fly an order of magnitude faster than the mean wind, Taylor's hypothesis is more easily fulfilled, so the length scales can be calculated by multiplying the measured time scale by the true airspeed.

Area source emission was measured using the airborne eddy covariance technique. Eddy covariance was used to directly measure fluxes of predetermined compounds. Because quadrupole systems analyze mass to charge ratios sequentially, only a small number of compounds can be selected for inclusion into the flux mode to keep the disjunct gap relatively small. The number of masses ranged from three to six during eight research flights. As the project was focused on California vegetation and in particular oak woodlands, isoprene (m/z 69) was measured on all the eight research flights, MVK + MACR (m/z 71) and methanol (m/z 33) on seven flights. Other VOCs measured on a smaller number of flights included monoterpenes (m/z 81, 137), MBO (m/z 87), acetaldehyde (m/z 45), benzene (m/z 79), toluene (m/z 93), and C8-aromatics (m/z 107). Spatially resolved eddy covariance fluxes were calculated using Wavelet

ACPD
14, 7965–8013, 2014

Analysis (Mauder et al., 2007) along flight tracks through the mixed layer. Since the majority of flights were conducted in the lower part of the mixed layer and the upper part of the surface layer (typically 150–300 m deep), we estimate the horizontal spatial resolution based on the blending height (e.g. Claussen M, 1990) using the surface layer scaling and the parameterizations for the mixed layer scaling (Karl et al., 2013).

2.6.1 Airborne virtual Disjunct Eddy Covariance (AvDEC)

The difference between virtual and conventional disjunct eddy covariance is that sampling flow is continuous but the dataset becomes disjunct because the quadrupole detector cycles through the m/z sequentially, producing regular gaps between high-frequency data points. For the small number of m/z scanned by the PTR-MS detector, AvDEC measurements are nearly equivalent to continuous AEC. In order to minimize the disjunct error the number of samples collected per integral scale and the effective duration of the sample period should be kept maximal. This can be achieved by limiting the number of m/z in the duty cycle and keeping the integration time long. We kept the number of VOC-related m/z between 3 and 6 at 0.1 s dwell time. In addition, on each flight, we monitored three control masses: hydronium ions (m/z 21), oxygen ions (m/z 32), and water vapor (m/z 37) at 0.1, 0.05, and 0.05 s, respectively, so the total cycle length varied from 0.5 to 0.8 s between different flights.

2.6.2 Fast Fourier Transform (FFT)

Fast Fourier Transform (FFT) is the conventional method to compute airborne flux. This method provides a single value for a given segment of flight, which limits the spatial resolution. The optimal integration stretch would be a sufficiently long pass to capture the optimal range of frequency distribution, but not so long that the turbulent structures are affected by diurnal effects. Therefore, resolution finer than 10 km would be challenging and uncertain using the FFT approach. Another challenge in this method is that it is

ACPD
14, 7965–8013, 2014

prone to non-stationarities. However, as an independent method it can be very useful for comparison with fluxes obtained from wavelet analysis (see Sect. 2.6.3).

2.6.3 Continuous Wavelet Transform (CWT)

Wavelet analysis, originally demonstrated to work with seismological data, has recently become increasingly popular in environmental and biological applications. Examples can be found in the analysis of the turbulent structures (Thomas and Foken, 2005; Mauder et al., 2007; Steiner et al., 2011; Metzger et al., 2013), and analysis of environmental processes at multiple scales (Stoy et al., 2009; Vargas et al., 2010).

The mathematic principle for the one-dimensional wavelet transform of a given signal $f(t)$ can be presented as:

$$T_p(a,b) = \int_{-\infty}^{+\infty} f(t)\overline{\Psi_{p,a,b}(t)}\mathrm{d}t, \tag{2}$$

where $T_p(a,b)$ are wavelet coefficients and $\Psi_{p,a,b}(t)$ is the wavelet function given by:

$$\Psi_{p,a,b} = \frac{1}{a^p}\Psi\left(\frac{t-b}{a}\right), \tag{3}$$

where $\Psi((t-b)/a)$ is termed "the mother wavelet", of which shape and locations are determined by the scale parameter of the wavelet a and by the translation parameter b. The normalization factor $1/a^p$ keeps the energy of the original mother wavelet (for $p = 1$). A general description of wavelet methodology can be found in Torrence and Compo (1998). For example, the Mexican-Hat mother wavelet works well with detection of single events, for example in the analysis of coherent structures of ejections and sweeps from a closed-canopy forest (Steiner et al., 2011). On the other hand, the complex Morlet function wavelet is suited to analysis of variance spectrum (Thomas and Foken, 2007). Nordbo and Katul (2013) looked at periodicities of long-term CO_2 fluxes

ACPD
14, 7965–8013, 2014

from soil. They showed that the intrinsic smoothing property of the wavelet produces results that are more easily interpretable, without the need of excessive manipulation of the original signal (e.g. averaging, smoothing, and tapering) or without restrictive assumptions (e.g. periodicity, stationarity).

The CWT method has an advantage over FFT in that it does not require homogeneity or stationarity, and can reconstruct the time domain to provide specific information on where in space/time and on which frequency the flux occurs. The wavelet flux method allows for the reconstruction of both the frequency and time domains of the flux within an integrated straight stretch of the desired length, and therefore can produce "instantaneous" or "discrete" fluxes which can be directly compared with model estimates. From the pragmatic point of view, integration of a stretch or a flight segment (e.g. of 100 km) results in not just a single flux value but delivers spatially resolved fluxes at discrete intervals sometimes informally referred to as instantaneous fluxes. Considering the footprint and wavelet scaling parameters, it is possible for an aircraft flying low at approximately 60 $m\,s^{-1}$ to provide meaningful spatial flux representation at the 1–2 km resolution needed for investigating landscape heterogeneity in high resolution biogenic emission models, although in principle even shorter intervals could also be resolved. An average of the wavelet fluxes can be compared to the Fourier flux from the same stretch. Given the independent approaches, the agreement between the methods adds to the confidence of the flux estimates and the ratio can be used as an additional measure of data quality. Finally the cross-spectra from the two methods can be compared. If no high-frequency attenuation losses exist, the cross-spectra should be similar. The wavelet approach can also be used for the correction of the FFT high-frequency spectral attenuation if it is related to tubing effects or factors other than the instrument response (Nordbo and Katul, 2013). Here, as the mother wavelet we used the Morlet wavelet. More detailed methodology of wavelet analysis used in this work has been presented by Karl et al. (2013) which was a further development from Karl et al. (2009). Vertical flux divergence of isoprene is expected to be primarily controlled due to its relatively short lifetime and was measured directly using "racetrack" profiles

ACPD
14, 7965–8013, 2014

at multiple altitudes. It was found to be linear and in the range 5 % to 30 % depending on the ratio of aircraft altitude to PBL height (z/z_i). We estimated the contribution of the storage term to the isoprene flux divergence to be of the order of 2–5 %, negligibly small compared to sensible heat fluxes. Fluxes were generally measured by flying consistently at 400 ± 50 m (a.g.l.) altitude, and extrapolated to the surface according to the determined flux divergence. The wavelet coefficients were optimized for the CWT analysis to perform well on stretches between 15 and 200 km with a typical ratio of FFT single flux value to CWT instantaneous flux average of between 1.0 and 1.3.

2.6.4 Flux footprints

The footprint for each flux point was derived using the Horst and Weil (1992) approach and depends on the wind speed, relative altitude to the PBL height, and the convective velocity scale.

Here we use scaling developed for the mixed layer according to:

$$\mathrm{d}x_{0.5} = 0.9\frac{u \cdot z_m^{2/3} \cdot h^{1/3}}{w^*}, \quad (4)$$

where $\mathrm{d}x_{0.5}$ is the half width of the horizontal footprint, u the horizontal windspeed, z_m the height above ground, h the PBL height and w^* the convective velocity scale which is derived from the wavelet heat flux in each transect.

The source contribution area can be approximated by projecting an upwind-pointed half dome with the $\mathrm{d}x_{0.5}$ parameter representing a radius of that half dome.

2.7 Error analysis (quality of fluxes)

As with eddy covariance on the ground, AEC fluxes must undergo a rigorous quality assessment, if not more so. The total uncertainty in reported airborne flux is the superposition of errors from calculation of concentrations (10 % for calibrated compounds

ACPD
14, 7965–8013, 2014

(5 % standard accuracy + 5 % dilution system), 30 % from relative lab-based sensitivity-relative transmission approach), survey-flight-specific random (5 %) and systematic (1 %) errors related to relative altitude within the PBL and to the aircraft leg, random error related to disjunct measurement (less than 1 %). For reactive tracers which require divergence corrections to yield the surface flux, uncertainty in PBL estimation (interpolated from saw-tooth soundings) is ±100 m which translates to 10 % of up to 30 % of the divergence correction, thus ∼ 3 %. We estimate the total accuracy for the reported surface fluxes to be 20 % for calibrated compounds and 40 % for other compounds.

The calibrated concentration data filtered for interferences (e.g. a biomass burning episode; see supplementary video) were used with corrected vertical wind speed data to derive covariance functions for each eligible stretch. The segments to be integrated (see example in Fig. 2) were selected based on constant roll angle of the aircraft between turns, and on consistency of altitude, excluding maneuvers with significant altitude changes such as soundings. Of segments prescreened for validity, only those with a clear peak in the covariance function (Fig. 3a) within the lag-time window of 5 s were accepted. The segment data were subsequently examined for similarities in the variances of concentration and vertical wind speed (Fig. 3b) together with the time series of wavelet frequency cross-spectra (Fig. 3c) within the cone of influence (COI) which is the region where the end of the power spectrum may be impacted by edge effects. Rather than excluding the part falling outside the COI, each of the ends of the time series are padded with zeros and excluded afterward, so the results are not affected by the COI. By comparing the wavelet cross-spectra with average cross-variance (Fig. 3d) it is possible to determine where in the wavelet period (inverse of frequency) the flux contribution occurs, enabling for example the visualization of the updrafts associated with high emissions.

Each stretch was finally analyzed for spectral characteristics, independently for the FFT and CWT methods (see Fig. 4). Identical procedures were applied to the fast temperature sensor for comparison. As the cross-spectra and ogives demonstrate, the VOC sampling system was not limited by high frequency attenuation owing to the short

ACPD
14, 7965–8013, 2014

0.1 s dwell time and small number of preselected VOCs in the quadrupole mass spectrometer cycle. It was found that the majority of the flux contribution (~ 90 %) was occurring between between 0.1 and 0.01 Hz which translates to the spatial scales of 0.6 to 6 km.

Additional quality measures were the ratio of the FFT and CWT fluxes (Fig. 5, upper panel), which for isoprene were usually 1 ± 15 % for survey transect flights. Identical values from the two methods were not expected as the FFT flux is affected by non-stationarities and inhomogeneities in contrast to the CWT flux, but the generally good agreement adds confidence to the results. Occasionally, a ratio higher than 1.15 was seen on short segments, or over a nonhomogeneous transect, or when the fluxes were close to zero. In sporadic cases when the fluxes were strongly non-stationary (characterized by the ratio higher than 1.3), the FFT flux was tagged as rejected and the CWT flux was only accepted if all the other quality criteria were fulfilled.

The generally good quality of fluxes in CABERNET was due to a combination of factors such as instrument sensitivities, response times, slow aircraft speeds and proximity to the source by flying at low altitudes (e.g. 400 m) and finally lack of spectral interferences (e.g. from propellers). Figure 5 (lower panel) shows the application of flux divergence (only reactive compounds such as isoprene) coefficients from racetrack profiling to derive the surface fluxes from the aircraft fluxes. In the remainder of the manuscript when discussing fluxes, we focus exclusively on the CWT fluxes due to the much higher spatial resolution of the flux and also because of their higher accuracy in cases with inhomogeneity and non-stationarity.

2.7.1 Simultaneous ground based measurements

Ground based measurements coinciding with aircraft passes in time and space were performed at two sites: The 525 m tall Hearst–Argyle Tower in Walnut Grove, California (WGC) located in the San Joaquin Delta region (38.2636, −121.4899, elevation 1 m) and the 23 m tall Tonzi Ranch Tower (TRT) (38.4308, −120.9656, elevation 177 m)

ACPD
14, 7965–8013, 2014

located in the relatively homogenous oak forest savannah between the Sierra Nevada foothills and the San Joaquin Delta.

Walnut Grove Tower

A PTR-MS was measuring vertical profiles of VOC concentrations at WGC as part of a separate study and we flew by the tower on RF 2 and RF 4 to take advantage of the opportunity to intercompare measurements. The vertical profile data from WGC also provides a broader perspective on the diurnal cycle and vertical distribution of BVOCs over California's Central Valley than can be obtained from the aircraft data which focused almost exclusively on midday and a specific altitude.

Briefly, the setup at WGC featured a PTR-MS analyzing air from 5 different heights (10, 131, 262, 394 and 525 m) for 2 min at each level per 10 min measurement cycle. There were 24 m/z monitored at 0.1 s dwell time each. The measurement footprint of the Tower increases with height and the top levels can pick up VOCs from the Central Valley's extensive agricultural, industrial, wetland, dairy, biomass burning and other activities from as far as the San Francisco Bay area hundreds of km away. The immediate vicinity of several km is mostly farmlands and wetlands with patchy biogenic sources constituted by mixed deciduous trees and broadleaf trees such as California Laurel (*Umbellularia californica*) therefore being only a small relative portion of the footprint at lower levels. The twin otter flew close to the tower on RF2 and more closely on RF4 (13:18) at 513 m (during an initial climb before the saw-tooth sounding) coinciding with the sampling of the tower at the top level (525 m) for which the intercomparison is shown in Sect. 3.1.5 and Supplement Fig. S2a.

Tonzi Ranch Tower

Tonzi Ranch tower is part of the long-term flux measurement network known as FLUXNET (Baldocchi and Ma, 2013; Baldocchi et al., 2006). During CABERNET, BVOC fluxes were measured for the first time at this site using a compact relaxed eddy

ACPD
14, 7965–8013, 2014

accumulation (REA) system custom built by NCAR and deployed at 23 m height to measure half-hourly flux data. The aircraft flew near the tower during RF2 and RF3. The closest flights which were compared passed right above the tower on 9 June at 11:41:15 at 280 m a.g.l., and on the returning leg on the same day at 13:33:19 at 410 m a.g.l.

3 Results and discussion

3.1 Observed Concentrations of BVOC from PTR-MS

The spatial distributions of VOC concentrations measured on most research flights are shown in Fig. 6. We show and discuss in this section the individual compounds measured in CABERNET in terms of their concentrations.

3.1.1 Isoprene

Isoprene concentrations were low, typically less than 50 ppt (0.05 mg m^{-2} h^{-1} in fluxes) in the Central Valley over agricultural terrains and over urban areas but were very high over the oak woodlands which cover approximately 7 % of California, and were the focus of the CABERNET campaign flight plans. In general, observed isoprene concentrations over oak woodlands ranged from less than 1 ppb on cool days up to several ppb on warmer flights. A maximum of 8 ppb was observed on the hottest day. The aircraft also saw marked increases of isoprene near some highways with eucalyptus trees planted alongside. Although no study of regional scale emissions of VOC in California was previously conducted, the pattern of concentrations observed during CABERNET is consistent with an expected pattern based on extrapolation of earlier studies from enclosures of dominant plant species of California which suggested oaks (mostly blue oaks), and to some degree eucalyptus trees, to be likely the most important isoprene emitters in California (e.g. Karlik and Winer, 2001). The broad range of temperatures encountered in different flights (mean range 21–33 °C) was responsible for quantitative

ACPD
14, 7965–8013, 2014

differences in concentrations over the overlapping segments. The actual concentration at the surface is expected to be significantly higher than observed at aircraft height, as is shown to be the case when flying near the tall tower at Walnut Grove where the top levels (394 and 525 m) saw very tiny concentration of isoprene consistent with the concentrations seen by aircraft although the lowest tower levels (10 and 131 m) saw much higher concentrations (Supplement Fig. S2b). However, the areas with significant biogenic emissions of isoprene covered a relatively small fetch within the footprint of the Walnut Grove tower.

3.1.2 Monoterpenes

Measurements of monoterpenes from aircraft are subject to several challenges which include (1) relatively small source strength, for example, ∼ 10 % relative to isoprene measured over coniferous regions; (2) relatively lower PTR-MS sensitivity compared to lighter compounds when using a quadrupole MS; (3) relatively shorter atmospheric lifetimes for some monoterpenes. The majority of the CABERNET aircraft tracks focused on isoprene emitters (e.g. oak woodlands) and not monoterpene emitters (e.g. coniferous forests), so the monoterpene signals were small and therefore we have not attempted to derive fluxes. However, averaging concentration signals to a 0.5 km resolution along the flight path was sufficient to decrease detection limits for monoterpenes to a few ppt and to demonstrate the presence of emissions from the densely forested areas, for instance, on a track towards Blodgett forest and on parts of the mixed conifer habitats along Coastal Ranges. Very high concentrations of monoterpenes exceeding 300 ppt were found in the GC cartridges on the flight legs passing near the Mojave Desert scrublands but m/z 81 and 137 were not included in ions measured by the PTR-MS on that flight.

ACPD
14, 7965–8013, 2014

3.1.3 Other VOCs

Although we focus on isoprenoids, the aircraft PTR-MS also measured concentrations (and fluxes) of other compounds with non-biogenic or partially biogenic sources such as dairies (methanol), isoprene photochemistry (MVK + MACR, hydroxyacetone), MBO to exclude interferences with isoprene, and sporadically other compounds such as acetaldehyde or aromatics. The data for these compounds are available and will be reported in other publications.

3.1.4 Inter-comparison of concentrations from PTR-MS and GC-MS

Measured concentrations of isoprene by GC-MS from cartridge samples collected at constant flow rate for 8 min during the flights generally agreed well with PTR-MS measurements averaged for the same periods, but there were occasional outliers most probably caused by cartridge sampling or analysis issues. The comparisons for each flight are presented in Supplement Fig. S3. Linear fits (excluding tubes which were found leaking or not sampled) ranged from R^2 0.79 for RF 1 (which was the flight with coldest weather and consequently lowest isoprene concentrations) to 0.98 for RF4, and was typically around R^2 0.9. The slope of the comparison ranged from 0.9 to 1.15 so within the combined measurement uncertainties (10 + 10 %). The analysis of the cartridges helped also in the exclusion of potential interferences at measured m/z.

3.1.5 Comparison with Walnut Grove Tower

WGC monitored VOC concentrations by a PTR-MS at 5 different heights (10, 131, 262, 394 and 525 m). The Twin Otter flew close to the tower on RF2 and RF4 (13:18). The ground-airborne comparison was focused on methanol, isoprene, and MVK + MAC. Overall, the comparison for methanol suggested agreement within 30 %. However, looking at simultaneous fine resolution data from the two PTR-MS instruments (Fig. S2a), a dip in methanol concentration was seen consistently by both the

ACPD
14, 7965–8013, 2014

aircraft and the tower when the plane was closest to the tower's top level, with excellent measurement agreement (11.6 ± 1.16 ppbv seen by the tower at 525 m vs. 11.9 ± 1.19 ppbv measured by the aircraft at 513 m). The variability of the methanol concentration over a five minute segment adjacent to the tower was within several ppbv, giving insight into spatial variability of methanol at that time and altitude. The WGC region is mostly agricultural with a variety of sparsely distributed trees. The measurement during the aircraft pass at 13:18 showed very little isoprene (below 50 ppt) at the top level of the tower (as mentioned in 3.1.1, and Supplement Fig. S2b) even though concentrations close to 1 ppb were observed at the 10 m level. The agreement for MVK + MAC (0.18 ± 0.02 ppbv aircraft vs. 0.20 ± 0.02 ppbv 525 m tower) was also good.

3.2 Observed fluxes

Isoprene and methanol showed the strongest fluxes of all measured compounds. In this paper we focus on reporting isoprene surface fluxes.

3.2.1 Isoprene fluxes

The observed surface emission rates of isoprene over oak woodlands ranged from around 1 to 15 $mg\,m^{-2}\,h^{-1}$. The measured isoprene flux distribution shown in Fig. 7 (CWT fluxes, 2 km resolution) visually confirms earlier predictions that isoprene emissions are almost exclusively produced by oak with a limited contribution from eucalyptus trees. For example, when entering the Sierra Nevada foothill oak band isoprene emissions rose remarkably above the low background in the Central Valley. Karlik and McKay (2002) used an isoprene emission factor from branch enclosure for blue oak of 27 $\mu g\,g^{-1}\,h^{-1}$, and leaf areas and weights from 14 blue oak trees from Sierra Nevada to estimate a leaf-level emission factor of ∼ 8 $mg\,m^{-2}$(leaf) h^{-1}, corresponding to a landscape emission factor of ∼ 4 $mg\,m^{-2}$(land) h^{-1} for a setting were oaks occupied half of the land surface area. In CABERNET the airborne emission factors for

ACPD
14, 7965–8013, 2014

isoprene over oak woodlands varied from less than 1 to ~ 10 mg m^{-2} h^{-1} with the average EF comprising all the flights over areas with oak presence (>= 20 % coverage of oak species according to GAP database) of 1.8 mg m^{-2} h^{-1}. However, the woodlands varied in species homogeneity, and more significantly, in the fraction (i.e., sparseness and patchiness) of tree coverage. It is necessary to emphasize that while the LAI of oak covered land surfaces has a relatively small range, about 3 to 6 m^2 m^{-2}, the fraction of the land surface covered by oaks can range from < 0.1 to 1. For example, Karlik and McKay (2002) using a precise method of calculating the areas of leaves from 14 trees divided by the areas of their crowns, measured an LAI of 4.3 m^2 m^{-2} for oak crown areas but the oaks only covered 42 % of the land surface resulting in an area average LAI of 1.8 m^2 m^{-2}. For the more sparse terrains the LAI can often be lower than 1 m^2 m^{-2}. Compared with the forests with closed canopies, modeling emissions from oak woodlands in California can be regarded as a specific case to which assessment by airborne flux measurements are particularly applicable. Measured airborne emissions reflect the true emissions from these California ecosystems of variable LAI ranging from less than 1 to about 5 m^2 m^{-2}.

3.2.2 Comparison of isoprene fluxes at Tonzi Ranch Tower

The aircraft flew over the Tonzi Ranch Tower twice, allowing two snapshot comparisons between the airborne CWT and ground based REA flux measurements. It is important to note that the airborne CWT averages over ~ 0.5 min (2 km), while the ground based REA averages over 30 min, and that the footprints related to each measurement are necessarily quite different, likely do not have the same oak biomass density, and thus the comparison is not expected to be perfect. In the first instance, the half-hourly REA flux was in excellent agreement with the 2 km average wavelet surface flux over the tower (i.e. 0.12 mg m^{-2} h^{-1} REA vs. 0.12 mg m^{-2} h^{-1} aircraft) while on the returning flight the ground based flux was 1/3 of the aircraft flux (i.e. 0.26 mg m^{-2} h^{-1} REA vs. 0.87 mg m^{-2} h^{-1}). Interestingly, the next half-hour REA flux was 0.96 mg m^{-2} h^{-1}, much

ACPD
14, 7965–8013, 2014

closer to the aircraft value. This may be due to a shift in wind direction and variability in oak biomass density around the tower but it should also be noted that the uncertainty in a single REA flux measurement is high and individual values are typically averaged to improve accuracy. These comparisons obviously suffer from significant uncertainties due to different footprints at different altitudes, different temporal coverage, and even temperature/PAR homogeneities. Nevertheless, the comparison provides insight about the variability in measurements at different scales, confirms observations at these scales are in a similar range, and indicates how airplane and tower measurements are complementary. A larger period of overlap in a future campaign is needed for gaining better statistics on such comparisons.

3.2.3 Comparison of isoprene emission factors to MEGAN landcover 2.2

Isoprene emission model estimates are based on basal emission rates, landcover characteristics, and the changes in emission associated with the environmental parameters temperature and photosynthetically active radiation (PAR). The airborne surface flux normalized for temperature and radiation using the Guenther et al. (2006) activity factor can be used to derive airborne basal emission factors (BEFs) to directly compare to emission factors used by models (e.g. the MEGAN emission factors version 2.2). A spatial comparison is shown in Fig. 7. It needs to be noted that such an approach introduces additional uncertainty from the temperature and PAR datasets and the algorithm used for calculating the activity coefficient, which are much higher than the uncertainty of the measured surface fluxes because of high sensitivity to errors in temperature and PAR. For this reason, in this manuscript we treat this comparison as semi-quantitative, and will explore this in more detail as part of another paper (Misztal et al., 2014) which focuses on using the airborne data to examine the accuracy of several different BVOC emission models, including detailed sensitivity analyses and input data validation. However, the qualitative picture clearly shows the remarkable correspondence of airborne BEFs derived at 2 km spatial resolution with landcover BEFs at a similar resolution. The transition from the low emitting environment in the Central Valley to highly emitting ar-

ACPD
14, 7965–8013, 2014

eas occupied by oak woodlands is clear (as shown earlier in Fig. 1). The most accurate match can be seen, for example, in the central part of the Sierra foothills and on the southern Coastal Range, to the south east of Monterey Bay and in the oak savannas near San Francisco Bay (Orinda, and Diablo Valley). The BEFs decline to zero over water bodies (e.g. San Francisco Bay, or lakes on the central-northern Sierras). There are some areas which do not agree well, for example, in the north-east over the Sierras which are dominated by conifers where airborne BEFs were somewhat lower. On the other hand, the areas where aircraft showed higher BEFs (e.g. beginning of RF8) are most likely related to inaccuracies in the oak landcover database.

4 Conclusions

We successfully made airborne eddy covariance flux measurements and mapped out horizontally varying source distributions of isoprene emissions for the dominant oak emitting ecosystems in California. The extensive oak woodlands in California are the most important regional source of isoprene which may be particularly relevant for air quality near heavily polluted regions of Central Valley. We observed high concentrations (up to 8 ppbv) and high surface emissions of isoprene ranging from several to more than ten mg $m^{-2} h^{-1}$ from the oak woodlands in the foothills of the Sierra Nevada and Coastal Ranges. Consistent with other studies we show that in the Central Valley isoprene emissions are typically undetectably small at aircraft level except for the areas of Eucalyptus trees planted near the highways. The temperature ranges in California cause changes in the isoprene emissions from relatively low to extremely high due to their strong temperature sensitivity. The ability of CWT for calculating fluxes at high spatial resolution (e.g. 2 km averaging) provides an optimal data set to compare BEFs from measurements with models. The data from this study will be used to assess isoprene emission-factor databases and isoprene emission response to landcover characteristics predicted for BVOC emission models.

ACPD
14, 7965–8013, 2014

Supplementary material related to this article is available online at http://www.atmos-chem-phys-discuss.net/14/7965/2014/acpd-14-7965-2014-supplement.zip.

Acknowledgements. We gratefully acknowledge California Air Resources Board (CARB) for funding CABERNET Contract #09-339, and the CIRPAS team for help in instrument integration. We acknowledge Abhinav Guha (UC Berkeley) for his contributions to the successful campaign. Finally, we would like to thank Andrew Turnipseed (NCAR) and Tiffany Duhl (NCAR) for performing GC analyses of aircraft cartridges, and Steve Shertz (NCAR) for engineering support. NCAR is sponsored by the National Science Foundation. Alex Guenther was partly funded under the Laboratory Directed Research and Development Program at PNNL, a multi-program national laboratory operated by Battelle for the US Department of Energy under Contract DE-AC05-76RL01830. We also acknowledge Maggi Kelly at GIF, UC Berkeley for suggestions regarding geospatial landcovers. We thank Jeremy Avise and Klaus Scott at California Air Resources Board for collaboration and useful modeling suggestions.

References

Apel, E., Riemer, D., Hills, A., Baugh, W., Orlando, J., Faloona, I., Tan, D., Brune, W., Lamb, B., and Westberg, H.: Measurement and interpretation of isoprene fluxes and isoprene, methacrolein, and methyl vinyl ketone mixing ratios at the PROPHET site during the 1998 Intensive, J. Geophys. Res., 107, ACH7-1–ACH7-15, doi:10.1029/2000JD000225, 2002.

Arey, J., Winer, A. M., Atkinson, R., Aschmann, S. M., Long, W. D., and Lynn Morrison, C.: The emission of (Z)-3-hexen-1-ol,(Z)-3-hexenylacetate and other oxygenated hydrocarbons from agricultural plant species, Atmos. Environ. A-Gen., 25, 1063–1075, 1991a.

Arey, J., Winer, A. M., Atkinson, R., Aschmann, S. M., Long, W. D., Morrison, C. L., and Olszyk, D. M.: Terpenes emitted from agricultural species found in California's Central Valley, J. Geophys. Res., 96, 9329–9336, 1991b.

ACPD
14, 7965–8013, 2014

Arey, J., Crowley, D. E., Crowley, M., Resketo, M., and Lester, J.: Hydrocarbon emissions from natural vegetation in California's South Coast Air Basin, Atmos. Environ., 29, 2977–2988, 1995.
Baker, B., Guenther, A., Greenberg, J., Goldstein, A. H., and Fall, R.: Canopy fluxes of 2-methyl-3-buten-2-ol over a ponderosa pine forest by relaxed eddy accumulation: field data and model comparison, J. Geophys. Res., 104, 26107–26114, 1999.
Baldocchi, D. D.: Assessing the eddy covariance technique for evaluating carbon dioxide exchange rates of ecosystems: past, present and future, Glob. Change Biol., 9, 479–492, 2003.
Baldocchi, D. and Ma, S.: How will land use affect air temperature in the surface boundary layer? Lessons learned from a comparative study on the energy balance of an oak savanna and annual grassland in California, USA, Tellus B, 65, 19994, doi:10.3402/tellusb.v65i0.19994, 2013.
Baldocchi, D., Tang, J., and Xu, L.: How switches and lags in biophysical regulators affect spatial-temporal variation of soil respiration in an oak-grass savanna, J. Geophys. Res.-Biogeo., 111, G02008, doi:10.1029/2005JG000063, 2006.
Desjardins, R. L., Hart, R. L., Macpherson, J. I., Schuepp, P. H., and Verma, S. B.: Aircraft-based and tower-based fluxes of carbon-dioxide, latent, and sensible heat, J. Geophys. Res.-Atmos., 97, 18477–18485, 1992.
Fares, S., Gentner, D. R., Park, J. H., Ormeno, E., Karlik, J., and Goldstein, A. H.: Biogenic emissions from Citrus species in California, Atmos. Environ., 45, 4557–4568, doi:10.1016/j.atmosenv.2011.05.066, 2011.
Fares, S., Park, J.-H., Gentner, D. R., Weber, R., Ormeño, E., Karlik, J., and Goldstein, A. H.: Seasonal cycles of biogenic volatile organic compound fluxes and concentrations in a California citrus orchard, Atmos. Chem. Phys., 12, 9865–9880, doi:10.5194/acp-12-9865-2012, 2012.
Fuentes, J. D. and Wang, D.: On the seasonality of isoprene emissions from a mixed temperate forest, Ecol. Appl., 9, 1118–1131, doi:10.2307/2641382, 1999.
Goldstein, A. H. and Galbally, I. E.: Known and unexplored organic constituents in the earth's atmosphere, Environ. Sci. Technol., 41, 1514–1521, 2007.
Goldstein, A. H. and Schade, G. W.: Quantifying biogenic and anthropogenic contributions to acetone mixing ratios in a rural environment, Atmos. Environ., 34, 4997–5006, 2000.

ACPD
14, 7965–8013, 2014

Goldstein, A. H., Goulden, M. L., Munger, J. W., Wofsy, S. C., and Geron, C. D.: Seasonal course of isoprene emissions from a midlatitude deciduous forest, J. Geophys. Res.-Atmos., 103, 31045–31056, 1998.

Goldstein, A., Hultman, N., Fracheboud, J., Bauer, M., Panek, J., Xu, M., Qi, Y., Guenther, A., and Baugh, W.: Effects of climate variability on the carbon dioxide, water, and sensible heat fluxes above a ponderosa pine plantation in the Sierra Nevada (CA), Agr. Forest Meteorol., 101, 113–129, 2000.

Guenther, A. B., Zimmerman, P. R., Harley, P. C., Monson, R. K., and Fall, R.: Isoprene and monoterpene emission rate variability – model evaluations and sensitivity analyses, J. Geophys. Res.-Atmos., 98, 12609–12617, 1993.

Guenther, A., Karl, T., Harley, P., Wiedinmyer, C., Palmer, P. I., and Geron, C.: Estimates of global terrestrial isoprene emissions using MEGAN (Model of Emissions of Gases and Aerosols from Nature), Atmos. Chem. Phys., 6, 3181–3210, doi:10.5194/acp-6-3181-2006, 2006.

Guenther, A. B., Jiang, X., Heald, C. L., Sakulyanontvittaya, T., Duhl, T., Emmons, L. K., and Wang, X.: The Model of Emissions of Gases and Aerosols from Nature version 2.1 (MEGAN2.1): an extended and updated framework for modeling biogenic emissions, Geosci. Model Dev., 5, 1471–1492, doi:10.5194/gmd-5-1471-2012, 2012.

Hegg, D. A., Covert, D. S., Jonsson, H., and Covert, P. A.: Determination of the transmission efficiency of an aircraft aerosol inlet, Aerosol. Sci. Tech., 39, 966–971, doi:10.1080/02786820500377814, 2005.

Horst, T. and Weil, J.: Footprint estimation for scalar flux measurements in the atmospheric surface layer, Bound.-Lay. Meteorol., 59, 279–296, 1992.

Jeong, S., Zhao, C., Andrews, A. E., Dlugokencky, E. J., Sweeney, C., Bianco, L., Wilczak, J. M., and Fischer, M. L.: Seasonal variations in N_2O emissions from central California, Geophys. Res. Lett., 39, L16805, doi:10.1029/2012GL052307, 2012.

Karl, T., Guenther, A., Turnipseed, A., Patton, E. G., and Jardine, K.: Chemical sensing of plant stress at the ecosystem scale, Biogeosciences, 5, 1287–1294, doi:10.5194/bg-5-1287-2008, 2008.

Karl, T., Apel, E., Hodzic, A., Riemer, D. D., Blake, D. R., and Wiedinmyer, C.: Emissions of volatile organic compounds inferred from airborne flux measurements over a megacity, Atmos. Chem. Phys., 9, 271–285, doi:10.5194/acp-9-271-2009, 2009.

ACPD
14, 7965–8013, 2014

Karl, T., Misztal, P. K., Jonsson, H. H., Shertz, S., Goldstein, A. H., and Guenther, A. B.: Airborne flux measurements of BVOCs above Californian oak forests: experimental investigation of surface and entrainment fluxes, OH densities and Dahmköhler numbers, J. Atmos. Sci., 70, 3277–3287, doi:10.1175/JAS-D-13-054.1, 2013.

Karl, T. G., Spirig, C., Rinne, J., Stroud, C., Prevost, P., Greenberg, J., Fall, R., and Guenther, A.: Virtual disjunct eddy covariance measurements of organic compound fluxes from a subalpine forest using proton transfer reaction mass spectrometry, Atmos. Chem. Phys., 2, 279–291, doi:10.5194/acp-2-279-2002, 2002.

Karlik, J. F. and McKay, A. H.: Leaf area index, leaf mass density, and allometric relationships derived from harvest of blue oaks in California oak savanna, USDA Forest Service General Technical Report Number PSW-GTR-184, Albany, CA, US Department of Agriculture, 719–729, 2002.

Karlik, J. F. and Winer, A. M.: Measured isoprene emission rates of plants in California landscapes: comparison to estimates from taxonomic relationships, Atmos. Environ., 35, 1123–1131, 2001.

Kuhn, U., Rottenberger, S., Biesenthal, T., Wolf, A., Schebeske, G., Ciccioli, P., Brancaleoni, E., Frattoni, M., Tavares, T., and Kesselmeier, J.: Isoprene and monoterpene emissions of Amazonian tree species during the wet season: direct and indirect investigations on controlling environmental functions, J. Geophys. Res., 107, LBA 38-1–LBA 38-13, doi:10.1029/2001JD000978, 2002.

Kurpius, M. R. and Goldstein, A. H.: Gas-phase chemistry dominates O_3 loss to a forest, implying a source of aerosols and hydroxyl radicals to the atmosphere, Geophys. Res. Let., 30, 24-1–24-4, doi:10.1029/2002GL016785, 2003.

Lamb, B., Westberg, H., and Allwine, G.: Isoprene emission fluxes determined by an atmospheric tracer technique, Atmos. Environ., 20, 1–8, doi:10.1016/0004-6981(86)90201-5, 1986.

Langford, B., Misztal, P. K., Nemitz, E., Davison, B., Helfter, C., Pugh, T. A. M., MacKenzie, A. R., Lim, S. F., and Hewitt, C. N.: Fluxes and concentrations of volatile organic compounds from a South-East Asian tropical rainforest, Atmos. Chem. Phys., 10, 8391–8412, doi:10.5194/acp-10-8391-2010, 2010.

Lenschow, D.: Probing the Atmospheric Boundary Layer, Probing the Atmospheric Boundary Layer, American Meteorological Society, Boston, MA, 1986.

ACPD
14, 7965–8013, 2014

Lenschow, D., Delany, A., Stankov, B., and Stedman, D. H.: Airborne measurements of the vertical flux of ozone in the boundary layer, Bound.-Lay. Meteorol., 19, 249–265, 1980.
Lenschow, D. H., Pearson, R., and Stankov, B. B.: Estimating the ozone budget in the boundary-layer by use of aircraft measurements of ozone eddy flux and mean concentration, J. Geophys. Res.-Oc. Atm., 86, 7291–7297, 1981.
Lenschow, D. H., Mann, J., and Kristensen, L.: How long is long enough when measuring fluxes and other turbulence statistics, J. Atmos. Ocean. Tech., 11, 661–673, 1994.
Loreto, F. and Sharkey, T. D.: A gas-exchange study of photosynthesis and isoprene emission in Quercus rubra L, Planta, 182, 523–531, 1990.
Mauder, M., Desjardins, R. L., and MacPherson, I.: Scale analysis of airborne flux measurements over heterogeneous terrain in a boreal ecosystem, J. Geophys. Res.-Atmos., 112, D13112, doi:10.1029/2006JD008133, 2007.
Metzger, S., Junkermann, W., Mauder, M., Butterbach-Bahl, K., Trancón y Widemann, B., Neidl, F., Schäfer, K., Wieneke, S., Zheng, X. H., Schmid, H. P., and Foken, T.: Spatially explicit regionalization of airborne flux measurements using environmental response functions, Biogeosciences, 10, 2193–2217, doi:10.5194/bg-10-2193-2013, 2013.
Moore, C.: Frequency response corrections for eddy correlation systems, Bound.-Lay. Meteorol., 37, 17–35, 1986.
Niinemets, Ü., Tenhunen, J., Harley, P., and Steinbrecher, R.: A model of isoprene emission based on energetic requirements for isoprene synthesis and leaf photosynthetic properties for Liquidambar and Quercus, Plant Cell Environ., 22, 1319–1335, 1999.
Nordbo, A. and Katul, G.: A wavelet-based correction method for eddy-covariance high-frequency losses in scalar concentration measurements, Bound.-Lay. Meteorol., 146, 81–102, doi:10.1007/s10546-012-9759-9, 2013.
Pankratz, D. and Bush, D.: Study of temporal and vertical ozone patterns at selected locations in California. Final report, AeroVironment, Inc., Monrovia, CA (United States), 1993.
Panofsky, H. A. and Dutton, J. A.: Atmospheric Turbulence: Models and Methods for Engineering Aplications, New York, Wiley, 1984.
Park, J.-H., Goldstein, A. H., Timkovsky, J., Fares, S., Weber, R., Karlik, J., and Holzinger, R.: Active atmosphere–ecosystem exchange of the vast majority of detected volatile organic compounds, Science, 341, 643–647, doi:10.1126/science.1235053, 2013.

ACPD
14, 7965–8013, 2014

Pattey, E., Strachan, I., Desjardins, R., and Massheder, J.: Measuring nighttime CO_2 flux over terrestrial ecosystems using eddy covariance and nocturnal boundary layer methods, Agr. Forest Meteorol., 113, 145–158, 2002.

Peischl, J., Ryerson, T. B., Holloway, J. S., Trainer, M., Andrews, A. E., Atlas, E. L., Blake, D. R., Daube, B. C., Dlugokencky, E. J., Fischer, M. L., Goldstein, A. H., Guha, A., Karl, T., Kofler, J., Kosciuch, E., Misztal, P. K., Perring, A. E., Pollack, I. B., Santoni, G. W., Schwarz, J. P., Spackman, J. R., Wofsy, S. C., and Parrish, D. D.: Airborne observations of methane emissions from rice cultivation in the Sacramento Valley of California, J. Geophys. Res.-Atmos., 117, D00V25, doi:10.1029/2012jd017994, 2012.

Pierce, T., Geron, C., Bender, L., Dennis, R., Tonnesen, G., and Guenther, A.: Influence of increased isoprene emissions on regional ozone modeling, J. Geophys. Res.-Atmos., 103, 25611–25629, doi:10.1029/98jd01804, 1998.

Rasmussen, R. A.: Isoprene: identified as a forest-type emission to the atmosphere, Environ. Sci. Technol., 4, 667–671, 1970.

Reid, J. S., Jonsson, H. H., Smith, M. H., and Smirnov, A.: Evolution of the vertical profile and flux of large sea-salt particles in a coastal zone, J. Geophys. Res.-Atmos., 106, 12039–12053, doi:10.1029/2000jd900848, 2001.

Reissell, A. and Arey, J.: Biogenic volatile organic compounds at Azusa and elevated sites during the 1997 Southern California Ozone Study, J. Geophys. Res.-Atmos., 106, 1607–1621, 2001.

Rinne, H., Guenther, A., Greenberg, J., and Harley, P.: Isoprene and monoterpene fluxes measured above Amazonian rainforest and their dependence on light and temperature, Atmos. Environ., 36, 2421–2426, 2002.

Rowe, M. D., Fairall, C. W., and Perlinger, J. A.: Chemical sensor resolution requirements for near-surface measurements of turbulent fluxes, Atmos. Chem. Phys., 11, 5263–5275, doi:10.5194/acp-11-5263-2011, 2011.

Schade, G. W. and Goldstein, A. H.: Fluxes of oxygenated volatile organic compounds from a ponderosa pine plantation, J. Geophys. Res., 106, 3111–3123, doi:10.1029/2000JD900592, 2001.

Schade, G. W., Goldstein, A. H., and Lamanna, M. S.: Are monoterpene emissions influenced by humidity?, Geophys. Res. Lett., 26, 2187–2190, 1999.

ACPD
14, 7965–8013, 2014

Schade, G. W., Goldstein, A. H., Gray, D. W., and Lerdau, M. T.: Canopy and leaf level 2-methyl-3-butene-2-ol fluxes from a ponderosa pine plantation, Atmos. Environ., 34, 3535–3544, 2000.

Scott, K. I. and Benjamin, M. T.: Development of a biogenic volatile organic compounds emission inventory for the SCOS97-NARSTO domain, Atmos. Environ., 37, S39–S49, doi:10.1016/S1352-2310(03)00381-9, 2003.

Serca, D., Guenther, A., Klinger, L., Vierling, L., Harley, P., Druilhet, A., Greenberg, J., Baker, B., Baugh, W., and Bouka-Biona, C.: EXPRESSO flux measurements at upland and lowland Congo tropical forest site, Tellus B, 53, 220–234, 2001.

Sharkey, T. D., Singsaas, E. L., Lerdau, M. T., and Geron, C. D.: Weather effects on isoprene emission capacity and applications in emissions algorithms, Ecol. Appl., 9, 1132–1137, 1999.

Steiner, A. L., Pressley, S. N., Botros, A., Jones, E., Chung, S. H., and Edburg, S. L.: Analysis of coherent structures and atmosphere-canopy coupling strength during the CABINEX field campaign, Atmos. Chem. Phys., 11, 11921–11936, doi:10.5194/acp-11-11921-2011, 2011.

Stoy, P. C., Richardson, A. D., Baldocchi, D. D., Katul, G. G., Stanovick, J., Mahecha, M. D., Reichstein, M., Detto, M., Law, B. E., Wohlfahrt, G., Arriga, N., Campos, J., McCaughey, J. H., Montagnani, L., Paw U, K. T., Sevanto, S., and Williams, M.: Biosphere-atmosphere exchange of CO_2 in relation to climate: a cross-biome analysis across multiple time scales, Biogeosciences, 6, 2297–2312, doi:10.5194/bg-6-2297-2009, 2009.

Thomas, C. and Foken, T.: Detection of long-term coherent exchange over spruce forest using wavelet analysis, Theor. Appl. Climatol., 80, 91–104, 2005.

Thomas, C. and Foken, T.: Flux contribution of coherent structures and its implications for the exchange of energy and matter in a tall spruce canopy, Bound.-Lay. Meteorol., 123, 317–337, 2007.

Torrence, C. and Compo, G. P.: A practical guide to wavelet analysis, B. Am. Meteorol. Soc., 79, 61–78, 1998.

Vargas, R., Detto, M., Baldocchi, D. D., and Allen, M. F.: Multiscale analysis of temporal variability of soil CO_2 production as influenced by weather and vegetation, Glob. Change Biol., 16, 1589–1605, 2010.

Westberg, H., Lamb, B., Hafer, R., Hills, A., Shepson, P., and Vogel, C.: Measurement of isoprene fluxes at the PROPHET site, J. Geophys. Res.-Atmos., 106, 24347–24358, 2001.

ACPD
14, 7965–8013, 2014

Winer, A. M., Arey, J., Atkinson, R., Aschmann, S. M., Long, W. D., Morrison, C. L., and D. M. Olszyk.: Emission rates of organics from vegetation in California's Central Valley, Atmos. Environ. A, 26, 2647–2659, 1992.
Wyngaard, J. C. and Brost, R. A.: Top-down and bottom-up diffusion of a scalar in the convective boundary layer, J. Atmos. Sci., 41, 102–112, 1984.

ACPD
14, 7965–8013, 2014

Table 1. Selected flight parameter data specific to each research flight.

	RF1 8 Jun	RF2 9 Jun	RF3 10 Jun	RF4 14 Jun	RF5 15 Jun	RF6 16 Jun	RF7 20 Jun	RF8 21 Jun
Temperature close to the surface (2 m WRF) (°C)								
mean (median)	20.6 (21.5)	23.1 (23.8)	24.4 (25.3)	27.8 (28.6)	28.5 (29.4)	24.8 (25.4)	29.7 (30.3)	32.5 (33.4)
s.d.	3.21	3.21	3.46	2.88	3.24	3.96	2.64	3.54
min	11.3	10.9	11.4	11.7	12.2	11.8	12.1	11.7
max	25.9	28.0	29.6	32.1	33.8	31.4	34.9	37.2
5th percentile	14.4	17.1	17.7	23.4	22.6	16.8	26.0	27.0
95th percentile	24.6	27.1	28.5	31.1	32.3	29.6	32.4	36.0
Altitude (m a.g.l.)								
mean (median)	603 (437)	551 (449)	831 (685)	529 (470)	511 (489)	836 (721)	852 (730)	462 (396)
s.d.	436	309	575	233	193	461	565	210
min	127	119	126	209	127	55.3	50.0	160
max	2410	1830	2790	1720	1460	2610	1870	1540
5th percentile	251	266	285	301	278	291	289	268
95th percentile	1670	1300	2090	949	712	1640	1830	887
Relative humidity at aircraft altitude (%)								
mean (median)	49.9 (42.7)	51.1 (51.1)	45.5 (46.9)	46.5 (46.7)	35.1 (36.5)	31.1 (29.9)	33.7 (34.2)	28.9 (26.6)
s.d.	17.6	16.2	15.7	7.62	9.11	13.3	11.0	8.87
min	21.2	18.4	12.0	18.4	11.1	9.78	8.8	13.2
max	100	100	95.6	83.4	68.6	99.2	85.8	68.6
5th percentile	31.2	27.1	18.0	33.3	17.3	13.0	11.7	18.5
95th percentile	86.1	95.6	70.2	58.0	48.2	45.9	47.7	48.1
Other flight characteristics								
Take off time UTC (local/PDT)	17:30 (11:30)	18:15 (12:15)	18:10 (12:10)	18:05 (12:05)	18:00 (12:00)	19:05 (13:05)	19:05 (13:05)	18:55 (12:55)
Touchdown time UTC (local/PDT)	22:20 (16:20)	22.45 (16:45)	22:10 (16:10)	22:35 (16:35)	22:30 (16:30)	0:05 (18:05)	00:30 (18:30)	23:30 (17:30)
Flight focus	Survey	Survey	Survey, Racetrack	Survey	Survey	Racetrack	Racetrack	Survey
Total length (km)	983	908	802	896	875	1020	835	935
PBL height range (km)	0.9–2.8	1.4–1.7	0.8–1.1	0.4–1.9	1.1–1.1	1.6–1.7	1.2–1.2	0.7–1.4
VOC-related m/z measured (10 Hz)*	69, 33, 79, 93, 107	69, 71, 33, 81, 137, 87	69, 71, 75, 33	69, 71, 33, 81, 137, 87	69, 71, 33, 81, 137, 45	69, 71, 87	69, 71, 75	69, 71, 33, 137, 87

* m/z 21, 32, and 37 were also measured on every flight at 10, 20 and 20 Hz, respectively.

ACPD
14, 7965–8013, 2014

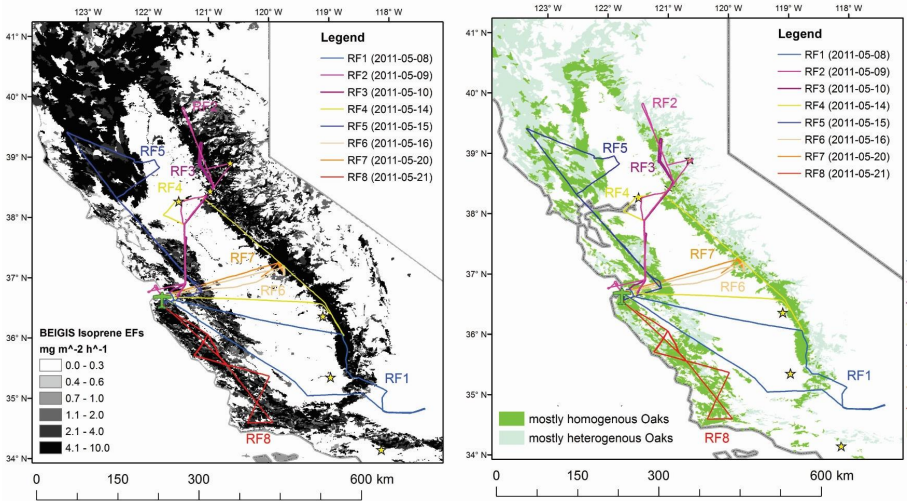

Fig. 1. Tracks flown during CABERNET overlaid over **(a)** BEIGIS Isoprene Emission Factor (EF) landcover; and **(b)** oak-woodland ecosystems differing in oak species spatial homogeneity (according to the GAP database).

ACPD
14, 7965–8013, 2014

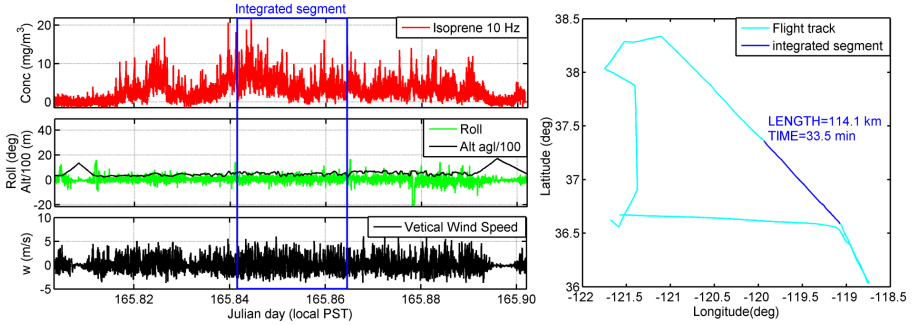

Fig. 2. Example of a segment integration based on roll to exclude turns and altitude to exclude large changes in altitude such as sawtooth soundings.

ACPD
14, 7965–8013, 2014

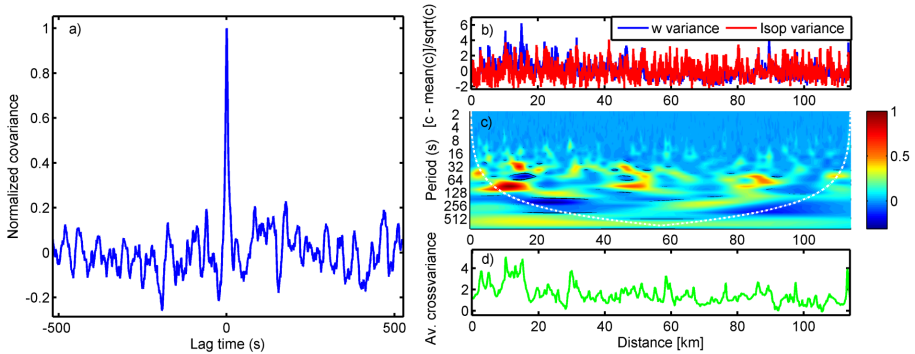

Fig. 3. Flux quality control for an example flight leg (the segment from Fig. 2). **(a)** Clear peak in the covariance function; **(b)** variances of w and isoprene; **(c)** time-resolved wavelet cross spectra; and **(d)** average cross-variance.

ACPD
14, 7965–8013, 2014

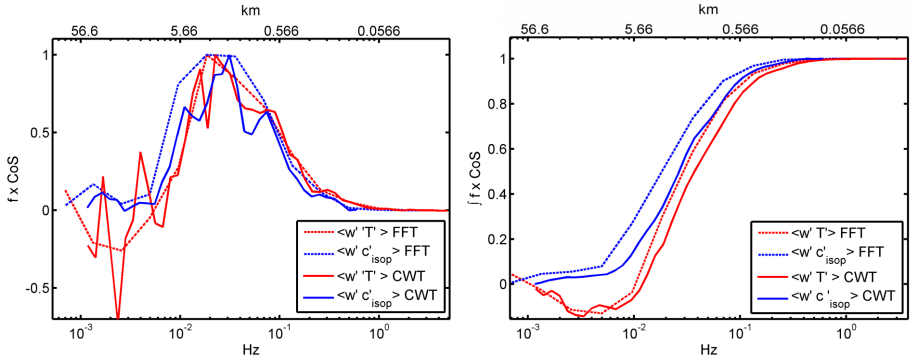

Fig. 4. Spectral quality control of the example flight segment. Left panel: Comparison of cross spectra for isoprene flux and heat flux using the FFT and CWT methods independently; Right panel: Cumulative cross spectra for isoprene flux and heat flux using the FFT and CWT methods independently.

ACPD
14, 7965–8013, 2014

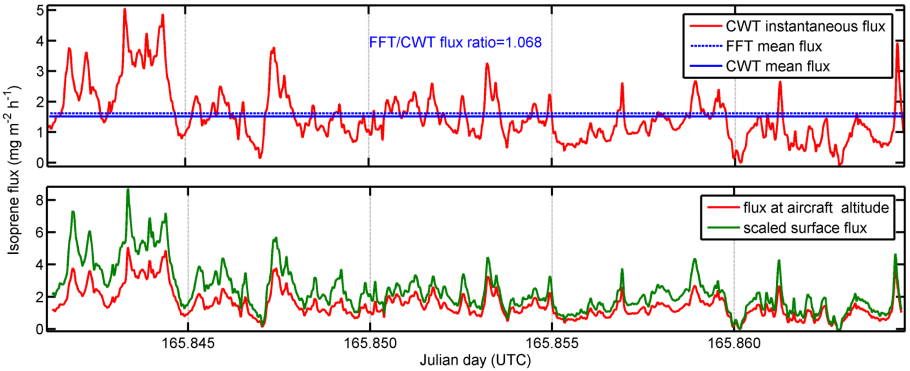

Fig. 5. Isoprene flux processing. Upper panel: determination of the FFT/CWT flux ratio; lower panel: application of flux divergence coefficients (derived in racetrack profiles) to scale fluxes from aircraft altitude to surface fluxes using aircraft altitude and PBL height.

ACPD
14, 7965–8013, 2014

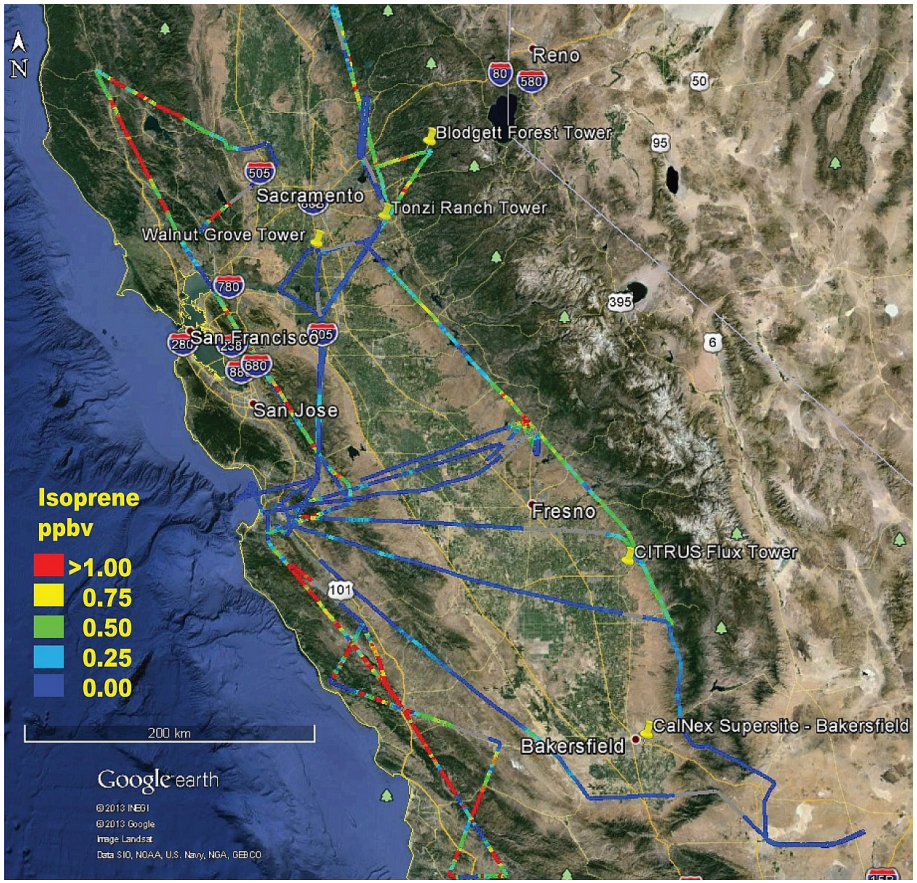

Fig. 6a. Spatial distributions of concentrations of isoprene.

ACPD
14, 7965–8013, 2014

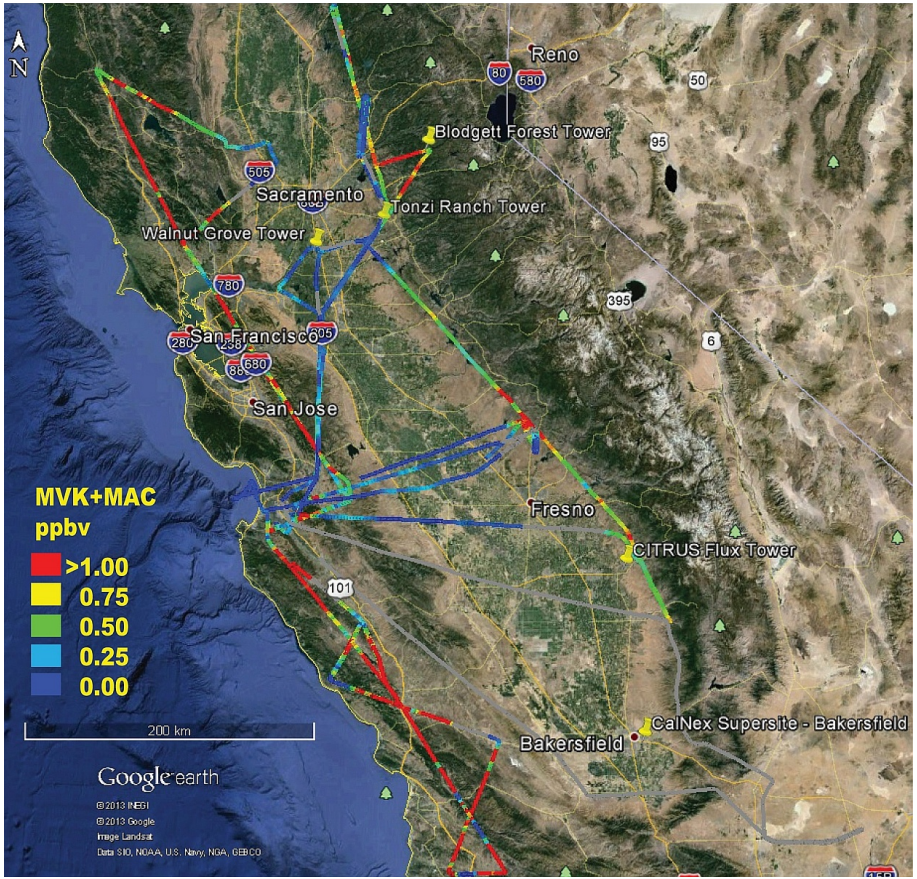

Fig. 6b. Spatial distributions of concentrations of MVK + MAC.

ACPD
14, 7965–8013, 2014

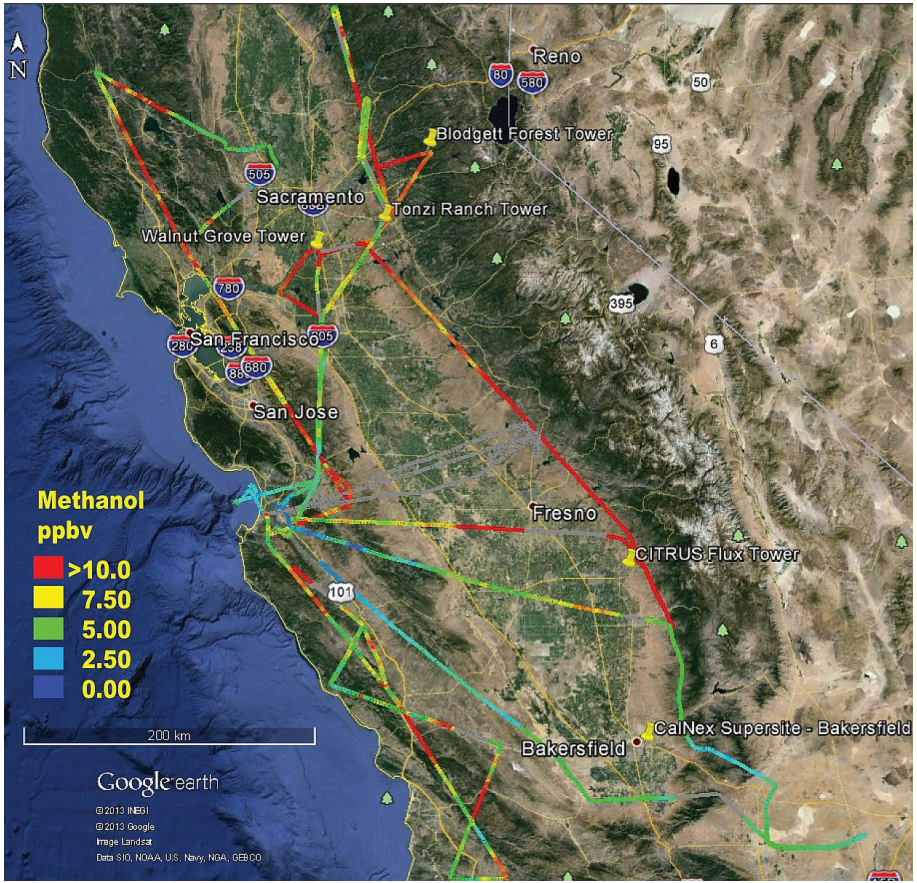

Fig. 6c. Spatial distributions of concentrations of methanol.

ACPD
14, 7965–8013, 2014

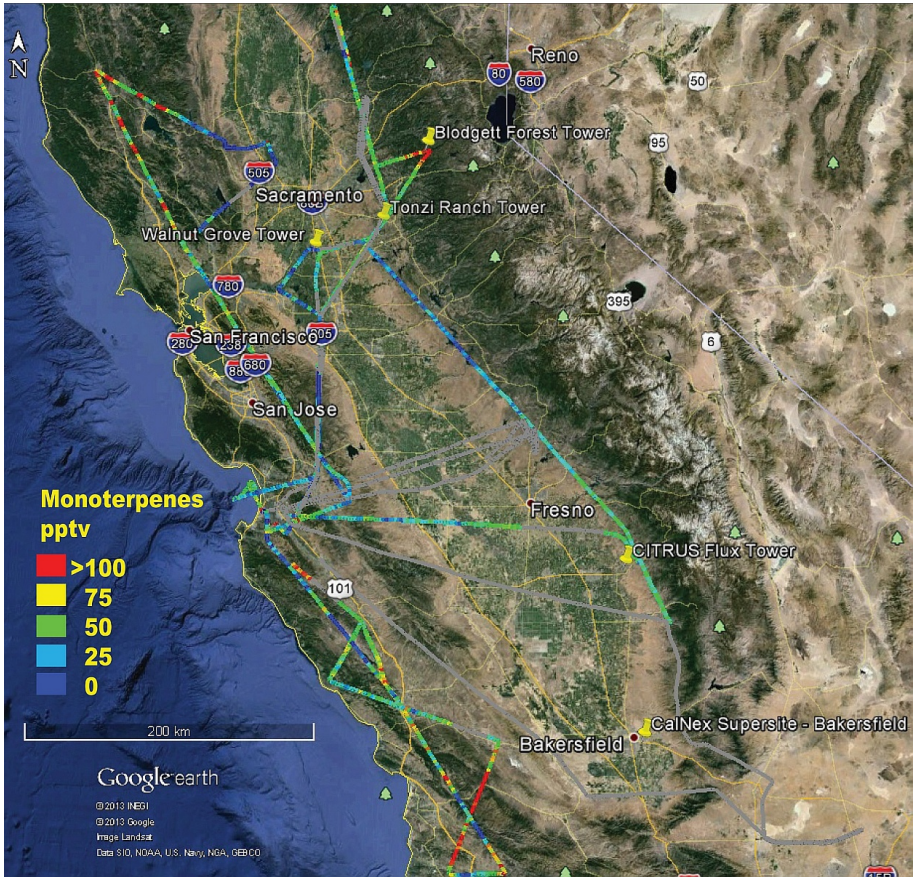

Fig. 6d. Spatial distributions of concentrations of monoterpenes measured during CABERNET.

ACPD
14, 7965–8013, 2014

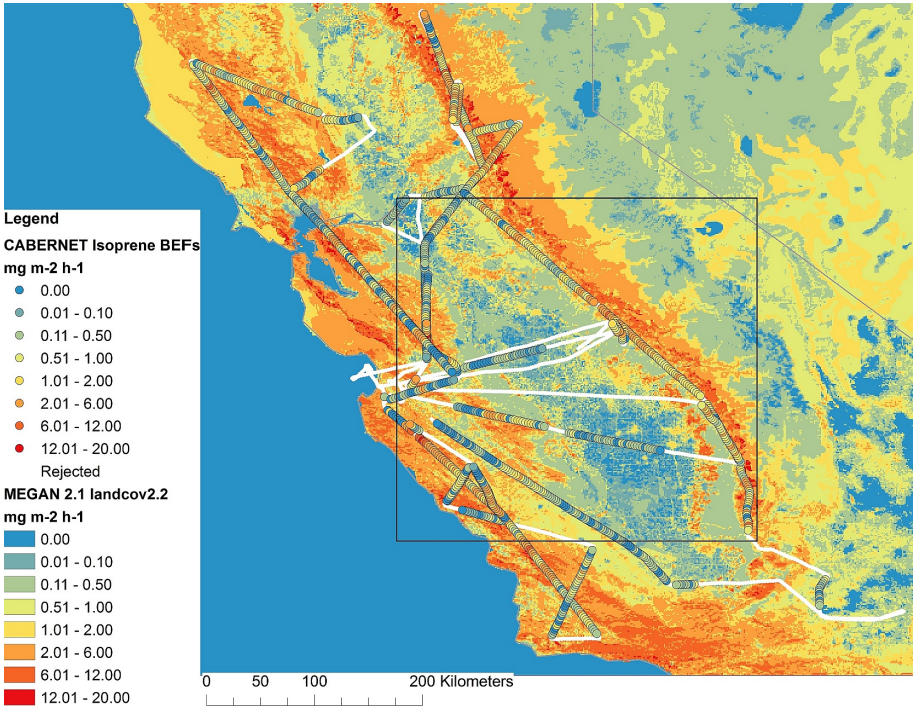

Fig. 7a. Comparison of airborne BEFs with MEGAN's landcover 2.2 for isoprene (airborne BEFs are subject to additional uncertainties introduced from T, and PAR and the algorithm's activity factor used in normalization). Full extent with a rectangle denoting.

ACPD
14, 7965–8013, 2014

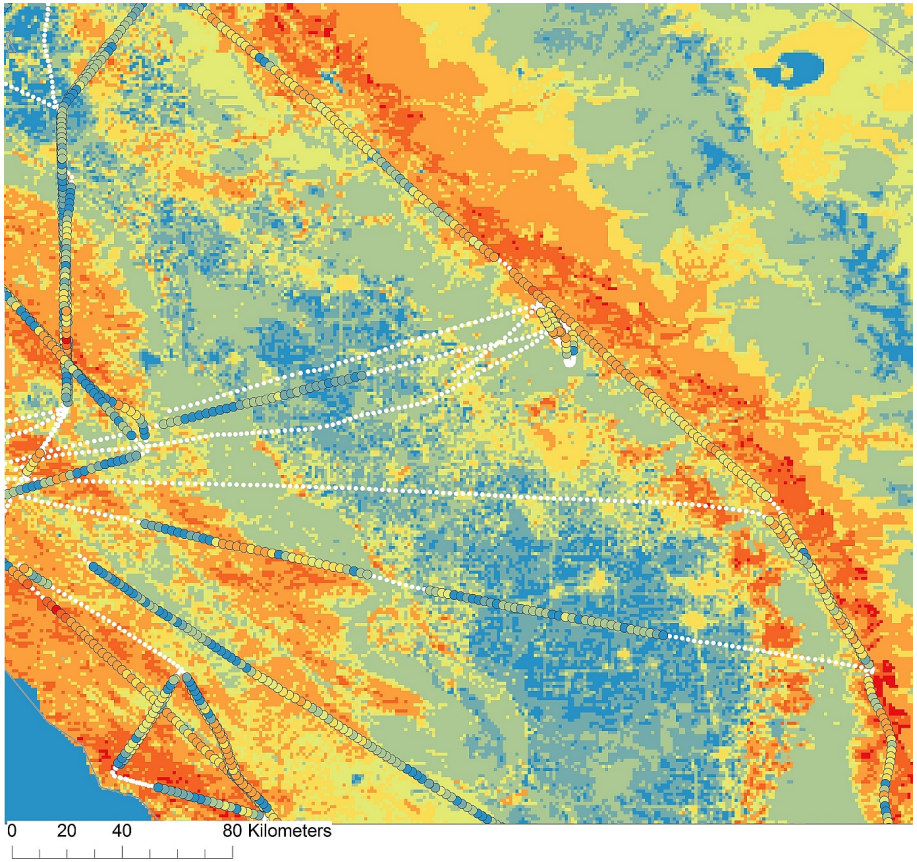

Fig. 7b. Same as Fig. 7a but with zoomed area.

ACPD
14, 7965–8013, 2014